J Bioenerg Biomembr (2013) 45:491–504
DOI 10.1007/s10863-013-9511-2

The inhibitors of antioxidant cell enzymes induce permeability transition in yeast mitochondria

Yulia Deryabina · Elena Isakova · Alexey Antipov · Nils-Erik L. Saris

Received: 4 April 2013 / Accepted: 5 April 2013 / Published online: 27 April 2013

Abstract In this study we investigated the effects of exogenous and endogenous oxidative stress on mitochondrial membrane permeability transition in yeast cells. *E. magnusii* yeast was used in the study as it is the only yeast strain possessing a natural high-capacity Ca^{2+} transport system. The key reactive oxygen species (ROS) detoxifying enzymes in the yeast cells - catalases (CATs) and superoxide dismutases (SODs) - were fully characterized. At least five isoforms of SODs and only one isoform of CATs were found in the *E. magnusii* mitochondria. The assessment of the main properties of mitochondrial non-specific permeability under physiological conditions such as dynamics of the membrane potential ($\Delta\Psi$) and swelling in mitochondria showed that under physiological conditions classical inhibitors of CATs (ATZ - 3-amino-1, 2, 4-triazole) and of SODs (DDC - diethyldithiocarbamate) caused irreversible decline in $\Delta\Psi$ in the yeast mitochondria. This decline was accelerated in the presence of 500 μM Ca^{2+}. The combined action of the inhibitors (ATZ + DDC) promoted moderate swelling in the isotonic medium, which was confirmed by transmission electron microscopy. Mitochondrial swelling in the cells exposed to antioxidant system inhibitors was accompanied by typical signs of early apoptosis, namely by chromatin margination and condensation, vacuolization of the cytosol, and damage of the plasma membrane. Here we showed, at both cellular and mitochondrial levels, that the deregulation of oxidant-scavenging enzymes directly leads to the opening of the mPTP, followed by induction of apoptotic markers in the whole yeast cells. Our studies are the first to clarify the highly contradictory data in the literature on mPTP in yeast mitochondria.

Keywords Ca^{2+} · Mitochondria · Yeast · Permeability transition pore · Antioxidant enzymes · Apoptosis

Abbreviations

$\Delta\Psi$	Mitochondrial transmembrane potential
AN	Adenine nucleotides
ALA	Alamethicin
ATZ	3-amino-1, 2, 4-triazole
CsA	Cyclosporin A
CATs	Catalases
CCCP	Carbonyl cyanide 3-chlorophenylhydrazone
DDC	Diethyldithiocarbamate
DMSO	Dimethyl sulfoxide
EtBr	Ethidium bromide
mPTP	Mitochondrial permeability transition pore
PBS	Phosphate saline buffer
P_i	Inorganic phosphate
PMSF	Phenyl-methyl-sulfonyl-fluoride
PCD	Programmed cell death
PI	Propidium iodide
$O_2^{\bullet-}$	Superoxide anion-radical
ROS	Reactive oxygen species
SODs	Superoxide dismutases
MetViol	Methylviologen
Rh123	Rhodamine 123
TEM	Transmission electron microscopy

Y. Deryabina · E. Isakova (✉) · A. Antipov
A.N. Bach Institute of Biochemistry, Russian Academy of Sciences, 119071, Leninsky pr. 33, Moscow, Russia
e-mail: elen_iss@mail.ru

Y. Deryabina
e-mail: yul_der@mail.ru

N.-E. L. Saris
Department of Food and Environmental Sciences, University of Helsinki, Viikki Biocenter 1, POB 56, 00014 Helsinki, Finland
e-mail: Nils.Saris@helsinki.fi

Introduction

The major ATP synthesis pathway in eukaryotes is mitochondrial oxidative phosphorylation (ox-phos). During the process the electrons are transferred from reducing substrates to O_2 via a chain of H^+-pumps, i.e. the respiratory chain complexes I-IV. Thus, an H^+-gradient across the inner mitochondrial membrane is formed and the complex V (ATP-synthase) utilises the electrochemical energy of the gradient for ATP synthesis (Nicholls and Ferguson 1992). Chemically, the stepwise reduction of O_2 ($O_2 \rightarrow O_2^{-\bullet} \rightarrow H_2O_2 \rightarrow OH^- \rightarrow H_2O$) proceeds via several reactive oxygen species (ROS). ROS are able to damage the key cellular components such as proteins, lipids and DNA, leading to pathologic cell states and apoptosis (Nicholls and Ferguson 1992; Halliwell and Aruoma 1991; Cabiscol et al. 2000; Perrone et al. 2008).

Mitochondria play a specific role not only in ATP synthesis but also in some other important metabolic processes. These include maintenance of cellular Ca^{2+} homeostasis (Gunter et al., 2000; Gunter et al., 2004), which affects numerous cell signaling pathways. Mitochondrial transport systems actively participate in changing the profiles of intracellular Ca^{2+} under both physiological and pathological conditions (Brookes et al. 2004). In turn, Ca^{2+} is a powerful physiological stimulus for ATP synthesis in mitochondria (McCormack and Denton 1994; Hansford and Zorov 1998). On the other hand, increase in intramitochondrial Ca^{2+}level, along with cellular ROS accumulation, mainly produced in mitochondria (Scherz-Shouval and Elazar 2011) leads to the opening of a non-specific Ca^{2+}-induced mitochondrial permeability transition pore (mPTP), release of cytochrome c and subsequent programmed cell death (PCD), i.e. apoptosis under pathological cellular conditions (Gulbins et al. 2003; Tsujimoto and Shimizu 2007; Kroemer et al. 2007). The Ca^{2+}-induced cyclosporin A (CsA)-sensitive pore is a multiprotein complex, which consists of an anionic channel through the outer membrane, an adenine nucleotides translocator and cyclophilin D (Crompton 1999; Rasola and Bernardi 2007; Leung and Halestrap 2008). Upon binding of Ca^{2+} under pathological conditions (e.g.,high temperature or oxidative stress, de-energization of mitochondria, depletion of intramitochondrial adenine nucleotide (AN) pools) this complex forms an open membrane pore of about 2.6–2.9 nm in diameter, capable of letting the low-molecular weight compounds of $M_r \leq 1500$ Da in and causing the release of accumulated Ca^{2+}, decrease in the membrane potential ($\Delta\Psi$) across the inner membrane and high-amplitude mitochondrial swelling (Crompton 1999; Rasola and Bernardi 2007; Leung and Halestrap 2008; Lemasters et al. 2009; Peng and Jou 2010; Azzolin et al. 2010). Currently, mPTP opening is considered as one of the channels for effective cation release from mammalian mitochondria under high cytoplasmic [Ca^{2+}] (Bernardi 1999) and as a pathway initiating key apoptosis reactions in animal cells (Gulbins et al. 2003; Tsujimoto and Shimizu 2007; Kroemer et al. 2007). Thus, in most eukaryotes, Ca^{2+} is not only a physiological but also a pathological effector (Herrero et al. 2008).

Unlike animal mitochondria yeast mitochondria are known to possess high resistance to Ca^{2+}-induced damage in membrane integrity (Kowaltowski et al. 2000; Deryabina et al. 2004; Yamada et al. 2009). Perhaps, it is related to the absence of high-capacity Ca^{2+} transport systems in most yeast mitochondria (namely, in *Saccharomyces serevisiae* and *Candida utilis*). But, on the other hand, a possible reason for such high resistance is a complex yeast antioxidant system, which protects the cells against oxidative stress inducing mPTP opening (Herrero et al. 2008; Kowaltowski et al. 2000; Kowaltowski and Vercesi 1999; Demasi et al. 2006). Catalases (CATs), superoxide dismutases (SODs), glutathione peroxidase and glutathione reductase should be mentioned among the key enzymes taking part in this process (Herrero et al. 2008; Lopez-Mirabal and Winther 2008). Mitochondria possess Mn^{2+}-dependent SOD, glutathione-peroxidase, glutathione-reductase, NAD(P)H transhydrogenase, thiolperoxidase (Kowaltowski et al., 2009). Moreover, there is a number of low-molecular weight compounds capable of deactivating ROS and maintaining redox balance in yeast (Herrero et al. 2008).

In one of the previous studies performed on the protoplasts from *S. cerevisiae* (Kowaltowski et al. 2000), formation of the Ca^{2+}-dependent membrane mPTP in the presence of the Ca^{2+}-ionophore ETH129 was described and it was induced by high [Ca^{2+}], thiol reagents and inhibition of antioxidant cellular systems, which in combination created the conditions for oxidative stress. In our previous study (Deryabina et al. 2004), we showed that the *Endomyces magnusii* mitochondria in spite of a powerful natural system of Ca^{2+} uptake and release (Bazhenova et al. 1998; Deryabina et al. 2001), demonstrate no mPTP under various conditions favorable for induction of this phenomenon. We have concluded that in this yeast species mitochondria either have no functional Ca^{2+}-induced mPTP opening or its regulation is quite different from those of animal mitochondria. Recently *Yamada* and co-authors (Yamada et al. 2009) have reported that under certain experimental conditions the *S. cerevisiae* mitochondria showed some signs of increased inner membrane permeability - such as high-amplitude swelling and cytochrome c release.

Some recent studies (e.g., Kovaleva et al. 2009; Trendeleva et al. 2011a; 2011b) have proved the absence of classical Ca^{2+}-dependent mPTP in the mitochondria from two yeast species of *Yarrowia lipolytica* and *Dipodascus*

(Endomyces) magnusii. Under conditions inducing membrane permeability transition some decline in $\Delta\Psi$ was observed only in the presence of the Ca^{2+} ionophore ETH129 if 30–50 μM Ca^{2+} was added to the *Y. lipolytica* mitochondria. It was not accompanied by any high-amplitude swelling and was insensitive to classical inhibitors of mammalian mPTP: CsA, Mg^{2+} and ADP, being partially restored by fatty acid, free BSA, phosphate inorganic (P_i), and ATP (Kovaleva et al. 2009). The authors concluded that some signs of mPTP opening could appear owing to induction of non-protein pore sensitive to Ca^{2+} and saturated fatty acids and suggested that this phenomenon may underlie formation of mPTP-like pore in yeast mitochondria. Of note, Trendeleva and co-authors (2011a) failed to detect pore opening in the mitochondria of both species under anaerobiosis, either. The combined action of various pro-oxidants such as diamide, t-butyl peroxide, phenylarsine oxide, oxaloacetate etc. was also ineffective (Trendeleva et al. 2011b). Thus, the ambiguity of available data impedes the understanding the nature and regulation of Ca^{2+}-dependent mPTP in yeast mitochondria. Despite extensive studies, the mechanism underlying transformation of redox disbalance in the yeast cell under endogenous stress into non-specific changes in mitochondrial membrane permeability and other distortions of cell physiology remains unclear.

Here, we used the *E. magnusii* yeast as the only yeast strain possessing a natural high-capacity Ca^{2+} transport system in order to elucidate the relationships between the change in membrane permeability and functioning of the antioxidant machinery in response to oxidative stress. Our data for the first time exposed (at both cellular and mitochondrial levels) the direct link between the regulation of oxidant-scavenging enzymes and mPTP opening and showed the role of these interactions in induction of apoptosis in the yeast cells.

Materials and methods

Yeast strain and culture conditions

The *E. magnusii* yeast was raised in batches of 100 ml in glycerol (0.6–1 %)-containing medium at 28° C as described previously (Deryabina et al. 2000). Cells were harvested in the exponential growth phase (10–13 g (wet weight)/l). To induce exogenous oxidative stress, the exogenous triggers were added into the cultivation medium at the mid-exponential stage. The concentrations of supplemented reagents were as following: menadione - 0.1–0.5 mM; methylviologen (MetViol) - 1–5 mM; H_2O_2 - 2–5 mM); 3-amino-1, 2, 4-triazole and (ATZ) - 2 mM; diethyldithiocarbamate (DDC) - 2 mM.

Isolation of mitochondria

Mitochondria were isolated according to the standard protocol described in (Bazhenova et al. 1998). Mitochondrial protein was assayed by Bradford method (Bradford 1976) with bovine serum albumin (BSA) as the standard.

Mitochondria were fully active for at least 4 h after preparation.

Respiration assessment

Oxygen consumption by the yeast cells was assessed *in vitro* at 25° C using electrodes covered by fluoroplastic film at a constant potential of 660 mV. The incubation medium contained 50 mM KP_i, pH 5.5, 1 % glucose. Analysis of respiratory activity was performed using a multichannel microelectrode polarograph with data-analysis software Record −4. Oxygen consumption in mitochondrial suspensions was monitored polaro-graphically with a Clark-type electrode in a medium containing 0.6 M mannitol, 1 mM Tris phosphate (pH 7.4), 1 mM EDTA, 20 mM pyruvate, 5 mM malate, and mitochondria corresponding to 0.4 mg protein/ml. All shown data traces are representative from four to six replicates.

Swelling of mitochondria

Mitochondrial swelling was monitored by recording changes in absorbance at 540 nm (A_{540}) with a Hitachi-557 spectrophotometer (Åkerman and Wikstrőm 1976) in medium containing 0.4 M mannitol, 0.2 M KCl, Tris-acetate, pH 7.4, 20 mM Tris-pyruvate, 5 mM Tris-malate, and 0.4 mg mitochondrial protein /ml. All shown data traces are representative of at least four replicates.

Mitochondrial membrane potential

$\Delta\Psi$ was measured in isolated mitochondria (0.4 mg protein/ml) at the wavelength pair of 511–533 nm using a Hitachi-557 spectrophotometer (Åkerman and Wikstrőm 1976) in incubation medium containing 0.4 M mannitol, 0.1 M KCl, 20 mM Tris-acetate, pH 7.4, 20 mM Tris-pyruvate, 5 mM malate, and 20 μM safranin. All shown data traces are representative of at least four replicates.

Preparation of the cellular homogenate

The cellular homogenate was obtained as follows: cells were twice washed with ice-cold water, resuspended in grinding medium (1:1 w/v).The medium contained: 10 mM MES, 0.5 M mannitol, 5 mM EDTA, and 0.5 mM phenyl-methyl-sulfonyl-fluoride (PMSF), pH 6.5. The yeast cells were disrupted with an ultrasonic disintegrator 9MSE (Farmacia,

Sweden) using some pulses at 0 °C for 2 min interrupted by cooling periods every 30 s. The obtained homogenate was centrifuged at 10,000 g for 30 min. The supernatant was used for the experiments.

Enzymes activities assay

Total CATs activity was measured polaro-graphically. Cellular suspension ($1-5\times10^8$ cells) was placed in 1 ml of 50 mM KP_i, pH 6.5, without substrate. The rate of oxygen emission was monitored after addition of 1 mM H_2O_2. Activity of CATs was calculated as the difference between the rates of oxygen emission in the presence of H_2O_2 and without any additions and was expressed in ng-atom $O_2\times min^{-1}$ g $^{-1}$ of dry weight. The activity of SODs was measured by monitoring the suspension at 406 nm (A_{406}) with a Specol-11 spectrophotometer (Germany) by inhibiting quercetin autooxidation as described in (Kostyuk et al. 1990). The procedure was performed in 20 mM KP_i buffer, pH 10.2, containing 0.8 mM TMDA, 0.1 mM EDTA, 1.4 μM quercetin. 50 % inhibition of quercetin autioxidation was considered as a SODs enzymatic activity unit.

Native analytical electrophoresis

Native analytical electrophoresis was performed as described by Davis (Davis 1964). We employed a 40 mA current in the separating mode. The CATs isozyms were visualized using the reaction between H_2O_2 and Fe^{3+} (Lledias et al. 1998). The electrophoresis SODs bands were visualized as follows: the gel was placed in water solution of tetrazolium blue (1 mg/ml) in the darkness for 20 min, then transferred to 20 mM KP_i buffer, pH 10.2, containing 0.8 mM TMDA (pH 10.8) and 1 mg of riboflavin and finally exposed to light until white spots against the dark background appeared.

Morphological identification of apoptotic changes in cells

Apoptotic changes in cells were visualized using staining of cellular chromatin by DAPI or by propidium iodide (PI) with a subsequent analysis using an Axioskop 40 FL fluorescence microscope (Zeiss). The cells were raised in the mid-exponential growth phase, fixed and permeabilized in 70 % (v/v) ethanol. Cells were then stained with DAPI solution (Streiblova 1988) and observed under the microscope. The fluorescent probe PI can permeate only through faulty membrane and dye the disintegrated DNA. As the negative cellular control we used untreated yeast cells. As the positive control we used the cells treated with the triggers agents and fixed in ethanol. Yeast cells were centrifuged at 4000 g for 10 min, resuspended in P_i saline buffer (PBS) containing PI (20 μg per ml), mixed gently, and incubated in the darkness at room temperature for 15 min. The cells were visualized with a fluorescence microscope (at 40× and 100×) using a blue filter.

Potential-depending staining

The energy state of the mitochondria was estimated by staining with a specific fluorescent potentiometric dye rhodamine 123 (Rh123). *E. magnusii* cells were grown to the mid-exponential growth phase. After ×2 washing yeast cells were incubated in the medium containing 0.5 μM Rh123 and examined after 0, 15, 20, and 30 min. The incubation medium contained 0.01 M PBS, and 1 % glycerol, pH 7.4. Preparations were examined under the Axioskop 40 FL microscope (Zeiss) at ×40 and ×100. To examine the Rh123-stained preparations, photofilters Zeiss no. 02, 15 were used (magnification ×100).

Transmission Electron Microscopy (TEM)

TEM analysis of untreated *E. magnusii* yeast cells (control) and of cultures, treated with inhibitors (DDC, ATZ) was carried out as described previously (Matrosova et al. 2009). Briefly, the yeast cells were raised in the mid-exponential phase of growth, precipitated, fixed with 2.5 % glutaraldehyde in 0.1 M sodium phosphate buffer (pH 7.2) for 2 h, and then post-fixed in 1 % OsO_4 for an hour at room temperature. After dehydration, the samples were embedded in Epon 812. Ultrathin sections were prepared with an LKB-8800 ultratome using diamond knives. Thereafter, the sections were stained with uranyl acetate for 60 min and post-stained as described previously (Reynolds 1963), and examined with a Jeol (JEM-100B) and Hitachi U-12 electron microscopes.

All the experimental data are expressed as means ± SEM, and statistical testing used the Student's t -test.

Results

Previously, we studied a wide range of conditions inducing endogenous oxidative stress (e.g., presence of a number of inhibitors and pro-oxidants, Ca^{2+} overload), and showed no mPTP development in the mitochondria of the *E. magnusii* yeast (Deryabina et al. 2004). No markers of PTP opening such as high-amplitude swelling, massive release of accumulated Ca^{2+}, decline in $\Delta\Psi$ were recorded. So, as the next step, here we attempted to promote mPTP by inducing exogenous oxidative stress with application of pro-oxidants and inhibitors of antioxidant system to the yeast culture in the mid-logarithmic phase of growth. The influence of H_2O_2 (Fig. 1a) and of the inhibitors of Cu/Zn-SOD (DDC) and of CATs (ATZ) (Fig. 1b), menadione and

MetViol (data not shown) were under investigation. Eventually, the growth of the *E.magnusii* yeasts occurred to be extremely resistant to addition of superoxide-producing agents such as menadione and MetViol. These pro-oxidants even at rather high concentrations (0.5 mM и 5 mM, respectively), caused only insignificant inhibition of growth rate. H_2O_2 at rather high concentrations (up to 5 mM) caused about 25 % growth inhibition, however, did not block it completely (Fig. 1a). On the other hand, addition of the inhibitors of the key antioxidant enzymes (DDC, ATZ) blocked the culture growth significantly (Fig. 1b). All attempts to isolate active mitochondria from the culture exposed to 2-hour treatment with the oxidants eventually failed. The results prompted us to analyze the key enzymes of cellular antioxidant system and to find out whether they play any role in mitochondrial membrane permeability regulation.

To evaluate antioxidant system of *E. magnusii* total enzymatic CATs and SODs activities in cellular homogenates, whole cells and mitochondria were analysed. Our data showed that the specific inhibitor of CATs, 4 mM ATZ, inhibited CATs activity nearly by 80 % whereas 4 mM KCN blocked it only by 60 %, which may be connected with peroxidases activities (Table 1). Native electrophoresis of CATs activity confirmed these findings. Fig. 2b, panel a, shows that cellular homogenates of *E. magnusii* visualized the only CAT isozym, which matched the standard cytosolic CAT of *Aspergillus niger* in activity (Sigma, USA) (Fig. 2a,

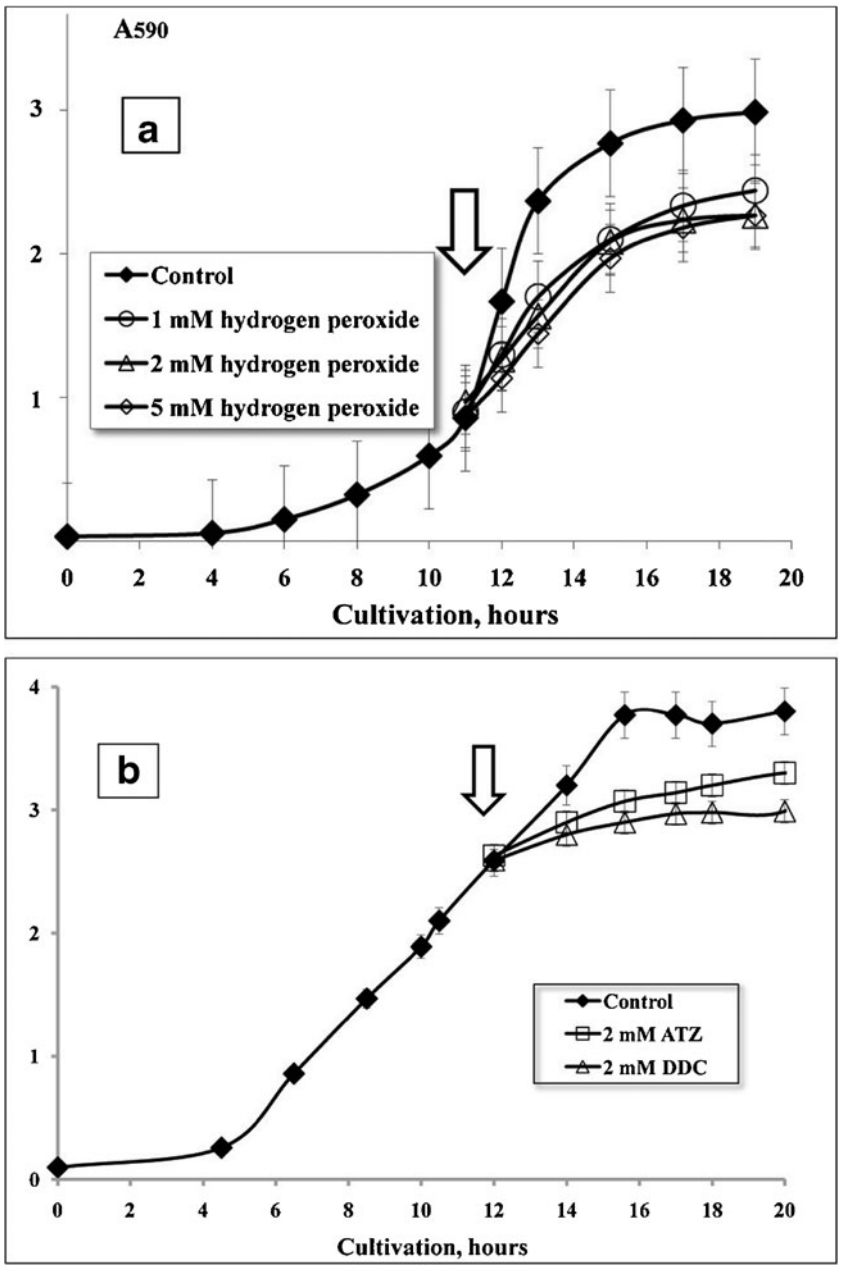

Fig. 1 Influence of oxidants and inhibitors of the antioxidant enzymes on the *E. magnusii* yeast growth in the mid-exponential phase. *Arrow* indicates the time of agent addition. **a** – **b** – application of: **a** – H_2O_2; **b** – inhibitors of the antioxidant enzymes 4 mM ATZ and 2 mM DDC. Experimental conditions are described in Materials and Methods

Table 1 Total activities of SODs and CATs of the *D. magnusii* yeast*

Enzyme	Control	Inhibition[a], % of the control		
		+ 4 mM ATZ[b]	+2 mM DDC[c]	+4 mM KCN
CATs activity, ng-atom of emitted O per 1 mg of dry weight	378.57	72.30–79.17	–	59.89
SODs activity, units of enzymatic activity per 1 mg of protein	121.16	–	57, 82–60, 27	59.41

[a] Description of experiments in Materials and Methods;

[b] 4 мМ ATZ was used as inhibitor of CATs;

[c] 2 мМ DDC and 4 мМ KCN are used as inhibitors of SODs

panel a). Pretreatment of the cells with 4 mM ATZ blocked the enzyme activity completely (Fig. 2c, panel a). The mitochondrial CATs also displayed the only distinct band with a molecular weight higher than that of the cytosolic one (Fig. 2d, panel a), which was fully blocked by 5 мМ ATZ (data not shown).

The activity of SODs was rather high and blocked by 2 mM DDC, a specific inhibitor of cytosolic SOD, by more

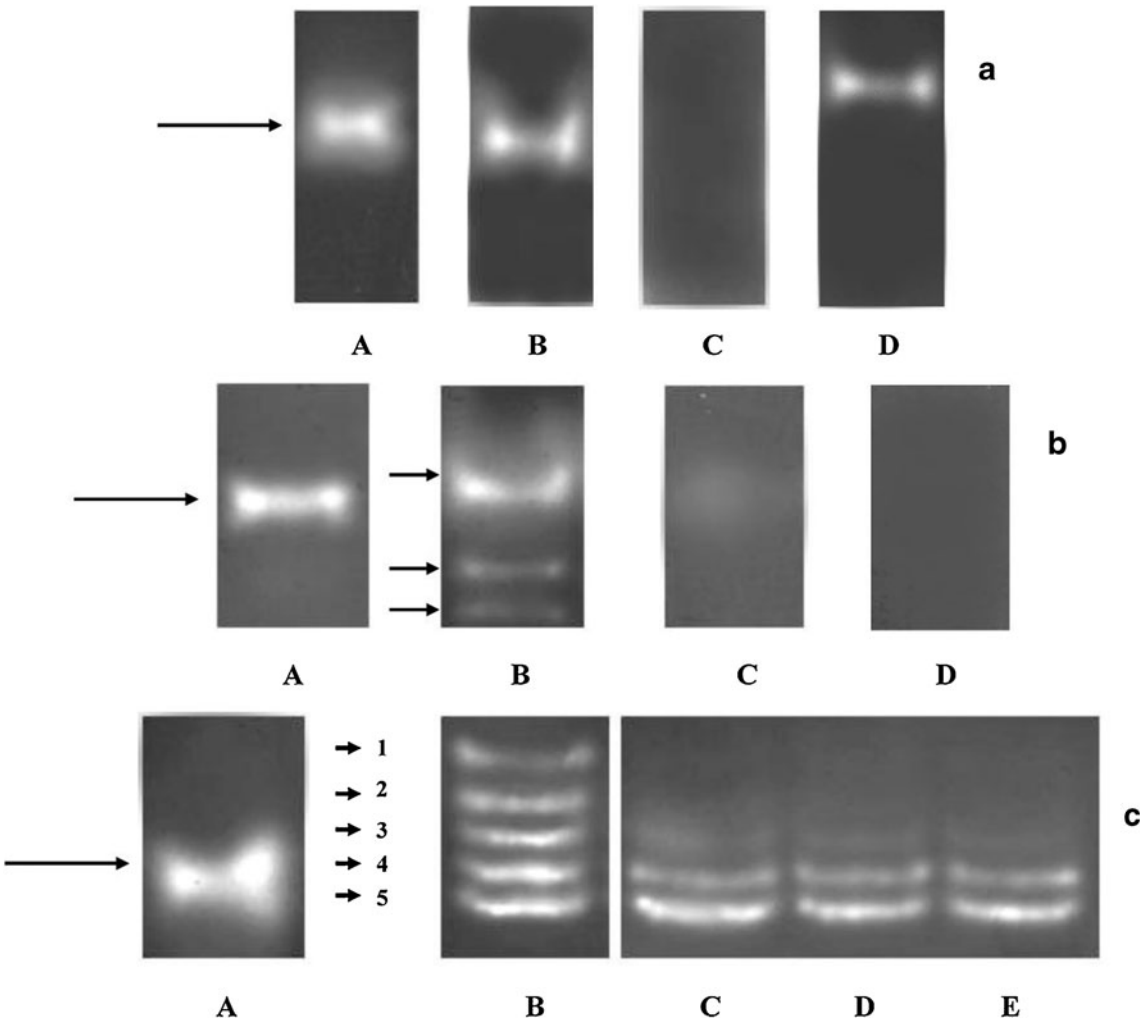

Fig. 2 Electrophoretic profiles of CATs and SODs activity of the *E. magnusii* yeasts. Panel **a**: *A* standard CAT from *Aspergillus niger* (Sigma); *B* cellular homogenate from the *E. magnusii* cells; *C* cellular homogenate treated with 2 mM ATZ; *D* mitochondria. Each sample contained 50 μg protein. *Arrow* indicates CATs activity. Panel **b**: *A* standard of Cu/Zn SOD from bovine erythrocytes (Sigma); *B* cellular homogenate from the *E magnusii* cells, control, normal conditions; *C* - *D* - cellular homogenate treated with: C - 2 mM DDC; D - both 2 mM DDC and 4 mM KCN. Each sample contained 15 μg protein. *Arrow* indicates SODs activity. Panel **c**: *A* standard of Cu/Zn SOD from bovine erythrocytes (Sigma); *B* mitochondria from the *E. magnusii* cells, control, normal conditions; *C* - *E* - mitochondria treated with: C - 2 mM DDC; D - 4 mM KCN; E - both 2 mM DDC and 4 mM KCN. Each sample contained 50 μg protein. Arrow indicates SODs activity

than 60 % (Table 1). To distinguish the activity of Cu/Zn-SOD (SOD1), located in the cytoplasm, from that one of Mn-SOD (SOD2), located in the mitochondrial matrix, the total enzyme activity was measured in the presence of KCN, which at low concentrations does not inhibit mitochondrial form, but blocks only SOD1 (Flohé and Otting 1984). As shown by Table 1 SOD1 isozym makes up to 60 % whereas SOD2 comprises the rest. Electrophoretic profiles of SODs in cellular homogenates (Fig. 2b, panel b) usually gave not fewer than three enzyme bands, the stronger band matched SOD protein from bovine erythrocytes (Fig. 2a, panel b) while two minor bands were of lower-molecular weight (Fig. 2b, panel b). The main isozym activity was significantly inhibited (nearly two fold) by 2 mM DDC (Fig. 2c, panel b) and totally blocked by the combined action of 2 mM DDC and 4 mM KCN (Fig. 2d, panel b). The analysis of mitochondrial SODs isozyms showed at least five enzyme bands (Fig. 2b, panel c) with different sensitivity to the inhibitors. 4 mM KCN (Fig. 2c, panel c) caused a complete inhibition of isozyms 1 and 2 and partially blocked isozym 3, but did not affect the activity of isozyms 4 and 5. 2 мM DDC affected the mitochondrial SODs isozyms in the similar way (Fig. 2d, panel c). The combined action of the inhibitors resulted in complete block of isozyms 1–3, but had no effect on isozyms 4 and 5 (Fig. 2e, panel c).

Next, we assessed the influence of the key antioxidant enzymes inhibitors at cellular and mitochondrial levels. All yeast mitochondrial preparations studied were highly intact as inferred from high respiratory rates in state 3 respiration (in the presence of ADP), metabolic state regulation upon successive additions of ADP, an average respiratory control ratio higher than 5, and ADP/O ratios being close to the theoretically expected maximum. The basic signs for non-specific changes in inner membrane mitochondrial permeability include: 1) decline in mitochondria $\Delta\Psi$; and 2) high-amplitude swelling of mitochondria due to uncontrolled entry of sugars and osmotically active compounds with a molecular weight of up to 1500 Da into the matrix, accompanied by subsequent water uptake. It suggests reduction of coupling, which may be caused by membrane damage. To investigate non-specific Ca^{2+}-dependent pore we assessed the changes in mitochondrial volume in the presence of Ca^{2+} and of CATs and SODs inhibitors. As it can be seen in Fig. 4, tightly coupled mitochondria could keep $\Delta\Psi$ constant for prolonged periods up to 600 sec. (Fig. 3a, *trace a*). The inhibitors of cytosolic CAT (ATZ, 4 mM), and of SODs (DDC, 2 mM) being applied in combination immediately declined $\Delta\Psi$ up to about 13 % of the original level with a subsequent slow but irreversible and insensitive to aeration decrease up to 50 % as early as after 300 s (Fig. 3a, *trace b*). If 500 μM Ca^{2+} was added 100 s before the inhibitors it caused the similar effect. However, the combined action of ATZ and DDC added after Ca^{2+} promoted more rapid decline in $\Delta\Psi$ (faster than after 120 s) and in contrast to the control it induced sudden and complete collapse of $\Delta\Psi$, which could be restored neither by aeration nor by any additions (Fig. 3a, *trace c*). If either ATZ (Fig. 3b) or DDC (Fig. 3c) were added to mitochondria separately it caused decline in $\Delta\Psi$ as early as after 400 s (Fig. 3b, *trace a*) and 30 s (Fig. 3c, *trace a*), respectively. Besides, in both cases dissipation of $\Delta\Psi$ was more than by 50 % (Fig. 3b, c, *traces a*). Intense aeration of mitochondrial suspension restored the membrane potential only for a short while with a subsequent irreversible collapse. The application of 500 μM Ca^{2+} into the incubation medium before the inhibitors of either CATs (ATZ, 4 mM), or of SODs (DDC, 2 mM) did not amplify membrane depolarization although $\Delta\Psi$ dissipated faster and in case of DDC, more completely (Fig. 3b, c, *traces b*). If 500 μM Ca^{2+} was added after the inhibitors it did not enhance their action (data not shown).

The energized mitochondria from *E. magnusii* manifested no high amplitude of swelling ($\Delta A = 0.1-0.9$) typical for mPTP in mammalian mitochondria, either at considerable concentrations of Ca^{2+} (1.25 nmols per 1 mg protein) or under the combined action of the inhibitors of antioxidant enzymes (Fig. 4a, *trace a*). We observed moderate-amplitude swelling induced by the Ca^{2+} uptake by mitochondria followed by water entry into the mitochondrial matrix. When ATZ and DDC were added into the medium 120 s after Ca^{2+} application they induced insignificant shrinkage of mitochondria up to about the initial volume (Fig. 4a, *trace b*). However, ATZ and DDC applied in combination into the incubation medium before Ca^{2+} apparently prevented decrease in turbidity of mitochondria suspension (Fig. 4a, *trace c*). Each of the inhibitors taken separately showed the similar results (data not shown).

The specific ultra-structure of the yeast mitochondria with much fewer and less developed crista than in the mammalian ones results in lower ability to stretch the inner membrane (Jung et al. 1997). This suggests that the maximal amplitude of swelling in yeast mitochondria should be much lower as compared to animal cells. To evaluate ability of the yeast mitochondria to swell we used an antibiotic alamethicin (ALA) (3.7 μg/ml), which being incorporated into mitochondrial membranes forms large pores with a diameter of 1 nm capable of passing through divalent cations and low molecular weight solutes, that is similar to Ca^{2+}-dependent mPTP. Figure 4b shows that ALA addition prompts the *E. magnusii* mitochondria to swell with a rather high amplitude of $\Delta A = 0.06$ that is considerably higher than the values in our experiments (Fig. 4a). Analysis of antioxidant system at both cellular and mitochondria levels and influence of its inhibitors on mitochondria properties promoted us to examine energy status and possible display of physiology damage in the whole yeast cells.

The early stages of cell programmed death (PCD) are known to be accompanied by dysfunctions of some mitochondrial processes, such as changes in $\Delta\Psi$ and alterations

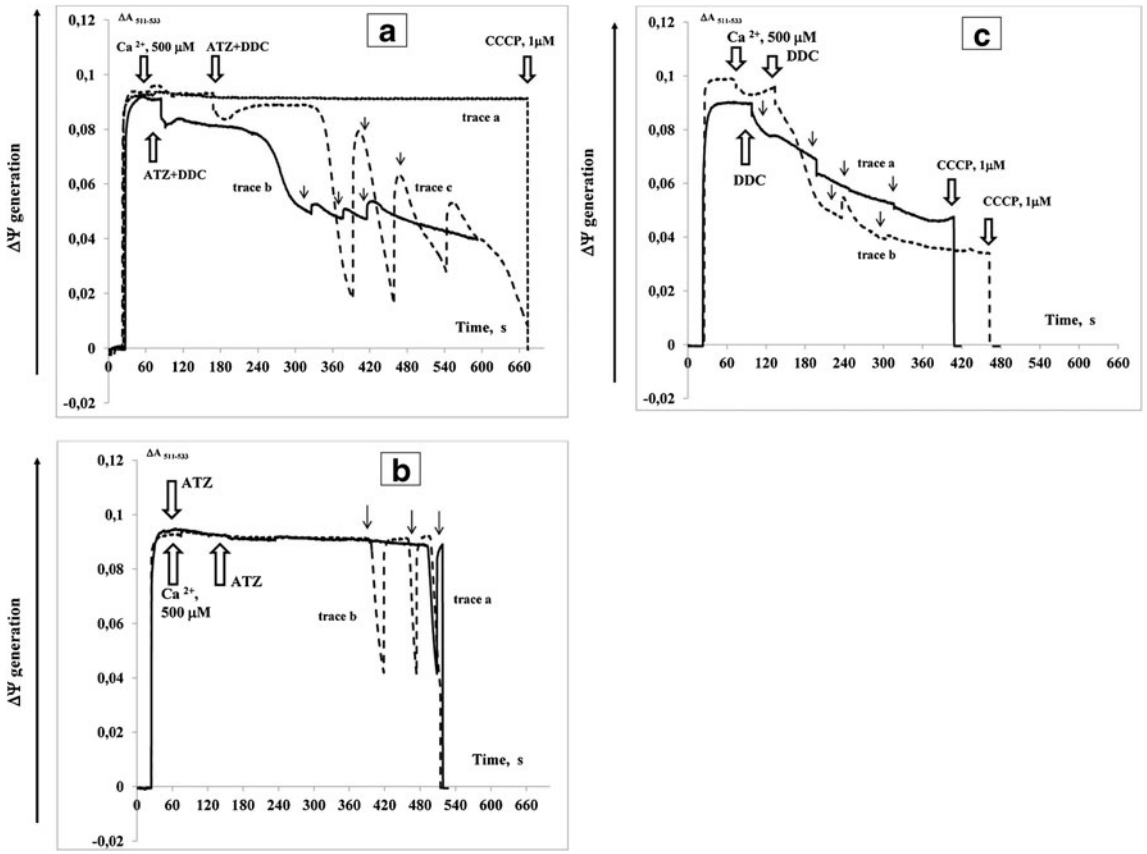

Fig. 3 Effects of Ca^{2+}, ATZ, and DDC on ΔΨ generated by the *E. magnusii* mitochondria respiring on pyruvate + malate. The incubation medium contained: 0.4 M mannitol, 0.1 M KCl, 20 mM Tris-acetate, and 0.4 mg of mitochondrial protein, pH 7.4. Additions and amounts are indicated by *large arrows*. Panel **a**: *trace a* - control; *trace b* - the membrane potential was dissipated by the combined action of 4 mM ATZ and 2 mM DDC; *trace c* indicates the results observed after the addition of 500 µM Ca^{2+} with decrease in ΔΨ when the ions are taken up followed by restoration. Panel **b**: *trace a* indicates the results observed after the addition of 4 mM ATZ; *trace b* indicates the results observed after the addition of 500 µM Ca^{2+} with subsequent application of 4 mM ATZ . Addition of 4 mM ATZ caused no decrease in ΔΨ. Panel **c**: *trace a* indicates the results observed after 2 mM DDC application; *trace b* indicates the results observed after the addition of 500 µM $Ca^{2+}$with subsequent 2 mM DDC application. *Small arrows* show when mitochondria suspension was stirred for aeration

in the oxidation-reduction potential due to induction of mPTP (Tsujimoto and Shimizu 2007). In order to detect the signs of early apoptosis, namely changes in the energy state of mitochondria, we used some specific fluorescent dyes such as Rhod123, MitoTracker Red CM-H2XRos and JC-1. Figure 5 shows data on Rhod123-stained yeast cells. As it is seen in fluorescent micro images (magnification ×100) the intact mitochondria in the energized *E. magnusii* cells are bright red, mainly rod-shaped (Fig. 5a). It indicates high energy cellular potential under these conditions. Pre-incubation of the *E. magnusii* cellular suspension with 0.5 – 1.0 mM Ca^{2+} caused no essential change in energy state of the cells (Fig. 5b). Analysis of energy state of the cells, pretreated with the oxidants and inhibitors of detoxifying enzymes for 30–60 min showed that most of the cells (about 90 %) were deenergized (Fig. 5c). The preliminary incubation of cells with 0.5 – 1.0 mM Ca^{2+} aggravated the effect (Fig. 5d). Moreover, the mitochondria looked smaller and round-shaped indicating their fragmentation. MitoTracker Red CM-H2Xros and JC-1 gave similar results (data not shown). Noteworthy, all the cells tested were negatively stained by PI thus implying the absence of necrotic damage of the cytosolic membrane and cellular physiology.

The apoptosis is well detected by DNA fragmentation and condensation of nuclear chromatin (reviewed by Kroemer et al. 2007). To verify apoptotic changes in the cells we visualized cellular nuclei using DAPI staining (Fig. 6). In control the nuclei were of distinctly round or similar shape, without any spots of chromatin (Fig. 6a, b). Treatment of the *E. magnusii* yeast with CATs and SODs inhibitors - ATZ and DDC - led to appearance of condensed chromatin in the nuclei and non-specific staining of cell cytosol (Fig. 6c, d), which could indicate abnormalities in cell physiology. However, neither of the inhibitors used separately gave similar effect (data not shown). Data on the ultra-structure of the *E. magnusii* cells pretreated with the antioxidant systems inhibitors in combination showed some dramatic changes in the cell morphology (Fig. 7b, d, f). Most of the cell population exposed to the

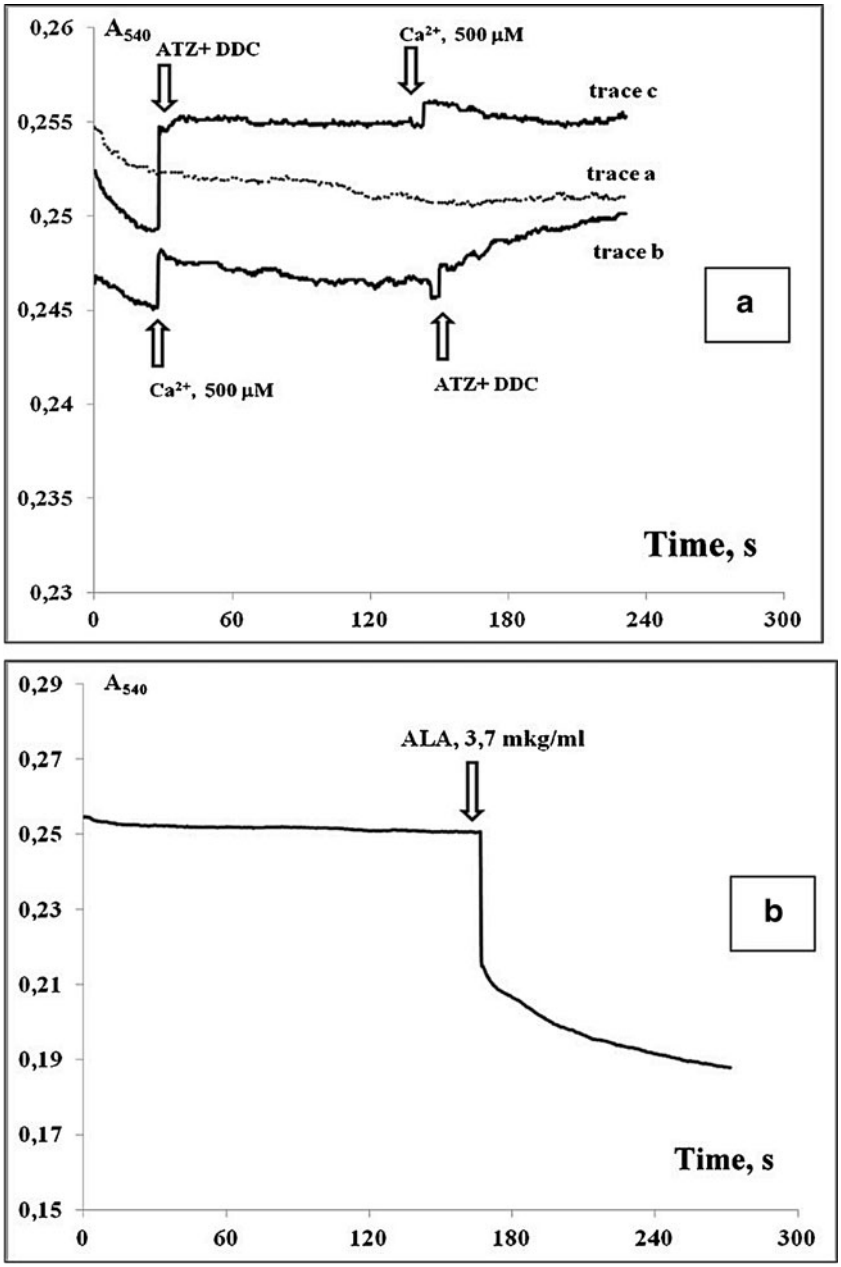

Fig. 4 The turbidity change in mitochondrial suspension was evaluated by measuring the absorbance at 540 nm. For this, yeast mitochondria were suspended in the incubation medium containing 0.4 M mannitol, 0.1 M KCl, 20 mM Tris-acetate, and 0.4 mg of mitochondrial protein, pH 7.4,. *Panel a* represents the results of turbidity change: *trace a* - control; *trace b* - induced by 500 μM Ca^{2+} application followed by the addition of antioxidant enzymes inhibitors - 4 mM ATZ and 2 mM DDC; *trace c* -induced by the addition of the inhibitors 4 mM ATZ and 2 mM DDC with subsequent addition of 500 μM Ca^{2+}. *Panel b* represents the results of turbidity change after ALA (3.7 μg/ml) addition into the medium

combined of ATZ and DDC showed vacuolization of the cytosol (Fig. 7b) typical for early apoptosis. Interestingly, the nuclei lost their distinct shapes and nuclear chromatin, which in normal cells takes up the central part of the nucleus, shifted to nuclear periphery (margination) and got fragmented. All these changes were even more obvious under high magnification (Fig. 7d). Mitochondria in control cells were of oval or cylindrical shape, electron-dense with evident crista structure (Fig. 7c, e). Being exposed to the antioxidant enzymes inhibitors they doubled in volume - from 0.48–0.54 μm up to 0.9–1.05 μm (Fig. 7e), which indicates swelling of the organelles under these conditions. In the micro images obvious changes in the mitochondria matrix structure, crista orientation and their deformation can be seen (Fig. 7e). Besides, most of the cells treated with the inhibitors of the oxidant-scavenging enzymes were characterized by plasma membrane damage and appearance of distinctive intrusions in it (data not shown). All these signs represent a definite signature of the apoptotic early stages in the cells exposed to the key antioxidant enzymes inhibition.

Discussion

In our study, the first attempt to link the function of antioxidant protective systems and mitochondrial activity to apoptotic processes in the *E. magnusii* yeast has been made. The systematic investigation into possibility of Ca^{2+}-

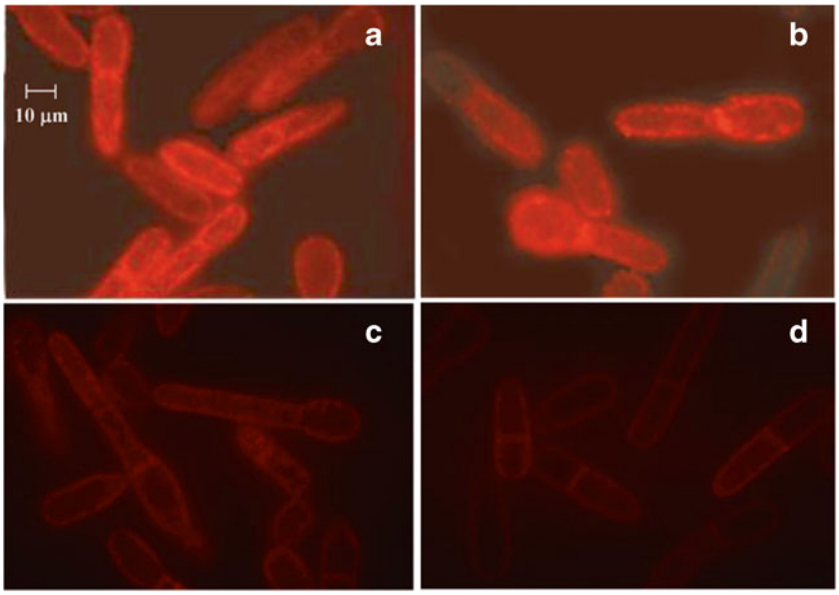

Fig. 5 Potential-dependent staining of mitochondria in the *E. magnusii* cells raised in the mid-exponential growth phase by Rh123. Cells were incubated with 0.5 μM Rh123 for 20 min. The incubation medium contained 0.01 M phosphate-buffered saline (PBS), 1 % glycerol, pH 7.4. The areas of high mitochondrial polarization are indicated by red fluorescence due to the concentrated dye. **a**, **b** - control, magnification 100×; **c**, **d** - cells were pre-treated with combined action of 5 mM ATZ and 5 mM DDC for 30 min, magnification 100×; **b**, **d** - incubation medium contained 0.5–1.0 mM Ca^{2+}. To examine the Rh123-stained preparations, filters 02, 15 (Zeiss) were used (magnification×100). Photos were taken using an AxioCam MRc camera

induced non-specific mPTP in the *E. magnusii* mitochondria was performed by our group before (Deryabina et al. 2004). Wide screening for the proper conditions for mPTP opening in the inner mitochondrial membrane showed that the mitochondria with a unique Ca^{2+} transport system including an actively functioning uniporter (Bazhenova et al. 1998) and a Na^{+}-independent pathway for accumulated cations release (Deryabina et al. 2001), are extremely resistant to high Ca^{2+} concentrations and manifest no typical mPTP markers (such as high amplitude swelling, decrease in ΔΨ and massive efflux of accumulated Ca^{2+}). In our previous studies high P_i concentrations (up to 10 mM) were used as a trigger to induce the non-specific pore opening (Deryabina et al. 2004). However, recently *Yamada* and co-authors (Yamada et al. 2009) found out that in *S. cerevisiae* mitochondria swelling due to 100 μM Ca^{2+} in the presence of the Ca^{2+} ionophore ETH 129 was inhibited by high [P_i].

Thus, we can conclude that yeast mitochondria display no typical properties of classical mPTP opening under the conditions of deenergization and depletion on intramitochondrial AN pools. It is well known that the Ca^{2+}-induced mPTP in mammalian mitochondria is maturing under certain pathological conditions due to imbalance between Ca^{2+} uptake through the plasma membrane and its efflux from the cell. Moreover, the critical increase in $[Ca^{2+}]_m$, stimulates the generation of ROS and free fatty acids, favorable for mPTP opening (Hajnyczky et al. 2006). In case of prolonged high cytoplasmic Ca^{2+} load, an open pore provokes non-specific high-amplitude mitochondrial swelling that finally causes release of proapoptotic mitochondrial agents and consequent cellular death (Azzolin et al. 2010). Jung and co-authors (Jung et al. 1997) postulated that in the *S. cerevisiae* yeast there is no classical mPTP, similar to animal mPTP. These authors had shown that yeast mitochondria are distinguished by a Ca^{2+}-independent, CsA-insensitive pore, which opens in the presence of ATP while oxidizing respiratory substrates. The phenomenon was named an mPTP of yeast mitochondria (YMUC). The key trigger of mPTP, P_i, inhibited high-amplitude swelling of yeast mitochondria. These results seem to be quite logical taking into consideration, that mitochondria from traditionally used yeast species (e.g., *S. cerevisiae* and *Candida utilis*) do not have a high-affinity system of Ca^{2+} accumulation (Carafoli et al. 1970; Balcavage et al. 1973). However, later *Kowaltowski* and co-authors (Kowaltowski et al. 2000), using digitonin-permeabilized protoplasts from both the wild type of *S. cerevisiae* and its mutants in thioredoxin peroxidase reported a drop in ΔΨ when high [Ca^{2+}] and some special agents such as phenylarsine oxide, P_i, and hydroperoxides were added. The protoplasts from the wild *S.cerevisiae* grown in the presence of CATs inhibitor displayed evident markers of mPTP. The authors suggested that generation of ROS in yeast cells makes them more sensitive to Ca^{2+}. Studies of the mitochondria from *Yarrowia lipolytica* and *E. magnusii* showed the decline in ΔΨ even at low [Ca^{2+}] (50–100 μM) but only in the presence of the Ca^{2+} ionophore ETH 129. This decline was partially inhibited by P_i and ATP (Kovaleva et al. 2009). These authors inferred that a non-specific mPTP of yeast mitochondria is not coupled to Ca^{2+} uptake and

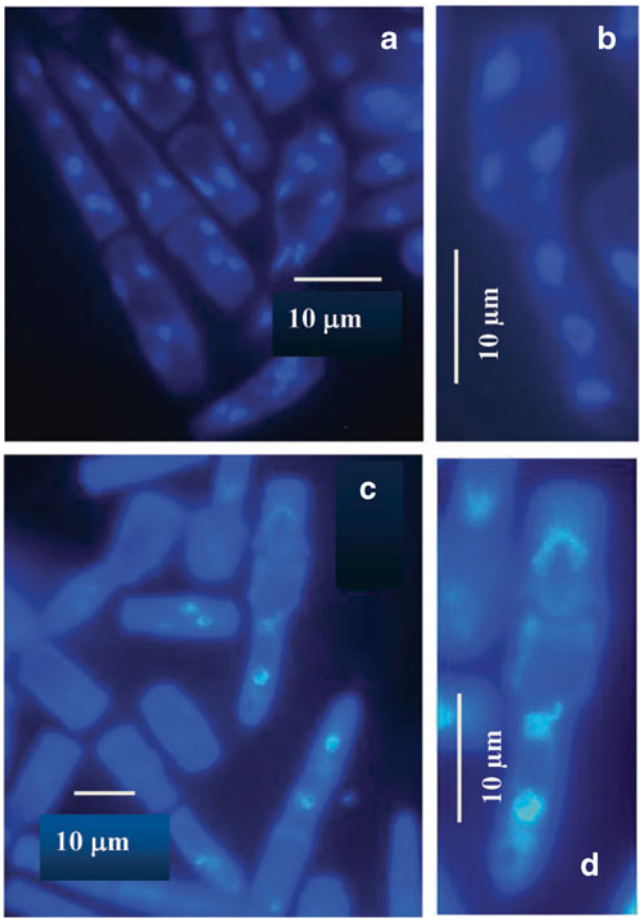

Fig. 6 Fluorescence micro-images of *E. magnusii* cells were raised in the mid-exponential growth phase and labeled with DAPI. Cells were stained for DNA using DAPI (300 nM in PBS) as described in Materials and Methods and examined under the fluorescence microscope (Zeiss). **a**, **b** - control cells (magnification 100×); **c**, **d** - cells were pretreated with the combined action of 5 mM ATZ and 5 mM DDC for 30 min, magnification 100×. Photos were taken using an AxioCam MRc camera

considerably differs from the classical and well-described mPTP. Lately *Yamada* and co-authors (Yamada et al. 2009) improved the procedure for detection of the specific pore markers and proved that CsA -independent Ca^{2+}-induced pore is present in the *S. cerevisiae* mitochondria. mPTP was promoted not only in the presence of exogenous NADH and ethanol as respiration substrates even without Ca^{2+}, but also at the combined action of 100 μM Ca^{2+} and ETH 129. The pore opening was inhibited by high [P_i] (10 mM). The correlation between exposure of mitochondria to Ca^{2+} and ultrastructural changes in organelles and slow release of cytochrome c was revealed (Yamada et al. 2009).

Our studies shed new light at the highly contradictory data on PTP in yeast mitochondria. The investigations into the main properties of non-specific permeability such as dynamics of ΔΨ and swelling in mitochondria showed that although the inhibitors of CATs and SODs, namely ATZ and DDC induced decline in membrane potential of the *E. magnusii* mitochondria (Fig. 3), their addition invoked no high-amplitude swelling in the isotonic medium (0.4 M манит, 0.1 M KCl) (Fig. 4). However, swelling amplitude considerably increased in the hypotonic medium (0.2 M mannitol, 0.1 M KCl) up to ΔA=0.02 (data not shown), which is similar to that one reported by *Yamada* and co-authors ((Yamada et al. 2009) on the *S. cerevisiae* mitochondria (ΔA=0.015) in the similar incubation medium (0.3 M mannitol) and at the similar mitochondria protein concentrations. Similarly to the data by *Yamada* and co-workers (Yamada et al. 2009), our TEM results showed that under the conditions of non-specific pore induction mitochondria volume significantly rises - not less than by 1.5 - 2 fold (Fig. 7f) most likely indicating mPTP opening. This phenomenon was confirmed at cellular level thus excluding the possibility of artifacts potentially invoked by the long procedure of mitochondria isolation when the organelles could change the volume and swell. Mitochondria swelling in the cells, exposed to the antioxidant system inhibitors, was accompanied by typical signs of early apoptosis such as chromatin margination and condensation, cytosol vacuolation, and damage of plasma membrane (Fig. 7b, d, f). *Ojovan* and co-workers (Ojovan et al. 2009) showed typical ultra-structural signs of early PCD without high-amplitude swelling of mitochondria (organelles volume double increased) when using an antiarrhythmic agent amiodaron as an inducer of apoptotic reactions in the *S. cerevisiae* yeasts. At the same time these authors demonstrated mitochondria fragmentation and distortion in space organization of mitochondrial reticulum. Based on the above-mentioned facts we suggest that the cardinal marker of mPTP development in the yeast mitochondria could be dissipation of ΔΨ causing further irreversible changes in mitochondria membrane permeability. The changes are expressed as mitochondria swelling with moderate or even low amplitude. Drop in ΔΨ studied was accelerated in the presence of Ca^{2+} (Fig. 3, *traces b*; Fig. 5b, d). The effect requires taking up the cation by mitochondria for its development. The results suggest that under certain conditions (in particular, when the cell antioxidant enzymes are blocked) PTP can be triggered in the *E. magnusii* mitochondria, which may not be Ca^{2+}-dependent but the pore is induced by Ca^{2+} ions.

Our data provide the first explanation of high resistance of the *E. magnusii* yeasts to external stress triggers (Fig. 1). This phenomenon is determined by active function of the key antioxidant enzymes- CATs and SODs. Yeasts possess an effective antioxidant system, the first line of which consists of CATs and SODs. Superoxide anion-radical ($O_2^{-\bullet}$) is the predecessor for most ROS and a mediator in the chain of oxidative reactions (Herrero et al. 2008). This free radical dismutation is activated by SODs which produce H_2O_2,

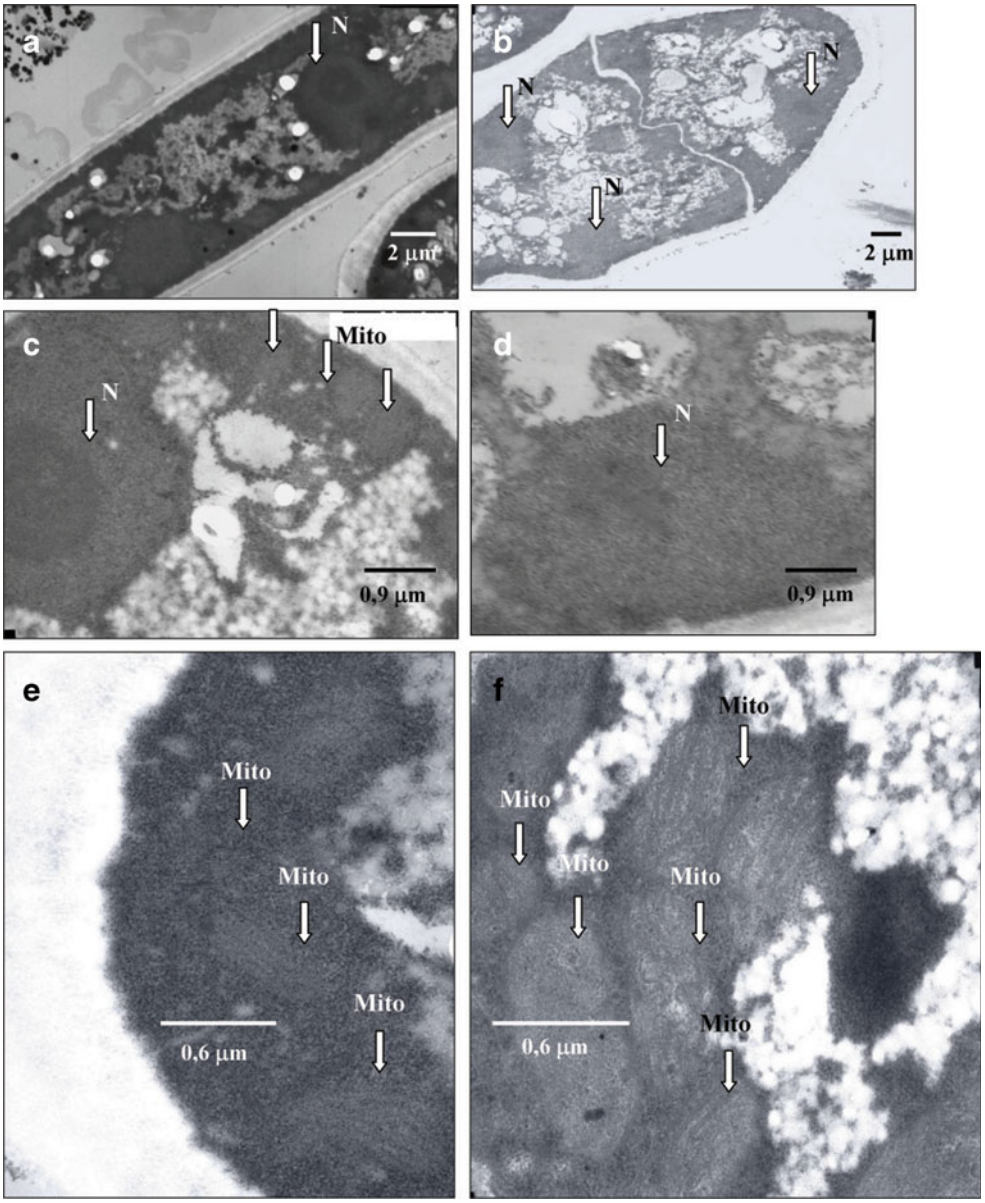

Fig. 7 Ultrastructure of the *E.magnusii* cells after 30 min incubation with inhibitors of CATs (5 mM ATZ) and SODs (5 mM DDC) (b, d, f) as compared to the cells under normal conditions (control) at the same magnification (a, c, e). N- nucleus, Mito - mitochondria. For details see Materials and Methods

being in turn reduced into H_2O by a number of CATs and peroxidases. In the *S. cerevisiae* yeast, two forms of SODs are known: Cu, Zn-dependent cytoplasmic SOD (SOD1) and Mn-dependent SOD (SOD2), located in the mitochondrial matrix (Lushchak, 2011). A certain fraction of SOD1 is assumed to be located in the inter-membrane space of mitochondria. Both SODs isozyms play a key role in detoxification of $O_2^{-\bullet}$, generated by the mitochondrial respiratory chain and diffusing into the inter-membranous space (Han et al., 2001). SOD1 takes an active part in yeast cell protection against external influence. It was shown that mutants in SOD1 are hypersensitive to $O_2^{-\bullet}$ produced by mitochondria. These mutants are either unable to grow under aerobic conditions at all or grow poorly, losing viability in the stationary growth phase, whereas SOD2-mutants display no hyper-sensitivity to exogenous oxidative stress (van Loon et al. 1986; Guidot et al. 1993; Costa et al. 1997). Our study showed that both the two oxidant-scavenging enzymes occur in both cytoplasmic and mitochondrial compartments (Fig. 2). Interestingly, in the *E. magnusii* mitochondria there is the only CAT isozym (Fig. 2d, panel a) and at least five SODs isozyms (Fig. 2c, panel c), two of them are blocked by classical inhibitors (Fig. 2c–e panel c). The nature of the other isozym bands requires further studies. Thus, our work revealed extremely high resistance of yeast mitochondria to Ca^{2+} overload under the conditions favorable for oxidative stress and mPTP opening. On the other hand, significant tolerance to external stress has been reported as a result of high activity of cell's antioxidant system. Based on these facts we conclude that the *E. magnusii* mitochondria are able to show evident markers of mPTP accompanied by distortion in cellular physiology,

however, this happens only if CATs and SODs activities are inhibited. *Yamada* and co-athors (Yamada et al. 2009) suggested that yeast mPTP being a phenomenon tightly connected with mitochondrial ability to take up Ca^{2+} may depend on the yeast species. Mitochondria from the species capable of active Ca^{2+} transport, such as *E. magnusii*, are likely to possess an adaptive mechanism providing their high resistance against Ca^{2+}-dependent mPTP opening. In this study, we demonstrated that this mechanism can underlie adaptive induction of extremely active antioxidant system. Cellular antioxidant enzymes are likely to play the cardinal role in protection of the *E. magnusii* mitochondria against the endogenous stress and Ca^{2+}-dependent mPTP.

Acknowledgments This study was supported by Russian Foundation for Basic Research (grants 08-04-01691-a, 09-04-90360 Yu-Oset-a) and Russian Ministry of Science and Education (grants No 11.519; 11.2010; 14.740; 11.01230). Dr. Saris is grateful for a grant from the Magnus Ehrnrooth Foundation in Helsinki. We thank Vera Teplova, Alexey Shevelev, and Olga Kamzolkina for help in discussion and critical reading of the manuscript.

References

Åkerman KEO, Wikström MKF (1976) Safranine as a probe of the mitochondrial membrane potential. FEBS Lett 68:191–197

Azzolin L, von Stockum S, Basso E, Petronilli V, Forte MA, Bernardi P (2010) The mitochondrial permeability transition from yeast to mammals. FEBS Lett 584:2504–2509

Balcavage WX, Lloyd JL, Matton JR, Ohnishi T, Scarpa A (1973) Cation movements and respiratory response in yeast mitochondria treated with high Ca^{2+} concentrations. Biochim Biophys Acta 305:41–51

Bazhenova EN, DeryabinaYI EO, Zvyagilskaya RA, Saris N-EL (1998) Characterization of a high-capacity calcium transport system in mitochondria of the yeast *Endomyces magnusii*. J Biol Chem 273:4372–4377

Bernardi P (1999) Mitochondrial transport of cations: channels, exchangers, and permeability transition. Phys Rev 79:1127–1155

Bradford MM (1976) A rapid and sensitive method for the quantitation of microgram quantities of protein utilizing the principle of protein-dye binding. Anal Biochem 72:248–254

Brookes PS, Yoon Y, Robotham JL, Anders MW, Sheu SS (2004) Calcium, ATP, and ROS: a mitochondrial love-hate triangle. Am J Physiol Cell Physiol 287:C817–C833

Cabiscol E, Piulats E, Echave P, Herrero E, Ros J (2000) Oxidative stress promotes specific protein damage in *Saccharomyces cerevisiae*. J Biol Chem 275:27393–27398

Carafoli E, Balcavage WX, Lehninger AL, Matton JR (1970) Ca^{2+} metabolism in yeast cells and mitochondria. Biochim Biophys Acta 205:18–26

Costa V, Amorim MA, Reis E, Quintanilha A, Moradas-Ferreira P (1997) Mitochondrial superoxide dismutase is essential for ethanol tolerance of *Saccharomyces cerevisiae* in the post-diauxic phase. Microbiology 143:1649–1656

Crompton M (1999) The mitochondrial permeability transition pore and its role in cell death. Biochem J 341:233–249

Davis BJ (1964) Disc electrophoresis. II. Method and application to human serum proteins. Ann NY Acad Sci 121:404–407

Demasi APD, Pereira GAG, Netto LES (2006) Yeast oxidative stress response. Influences of cytosolic thioredoxin peroxidase I and of the mitochondrial functional state. FEBS J 273:805–816

Deryabina YI, Bazhenova EN, Zvyagilskaya RA (2000) The Ca^{2+}-Transport system of yeast (*Endomyces magnusii*) mitochondria: independent pathways for Ca^{2+} uptake and release. Biochem Mosc 65:1352–1356

Deryabina YI, Bazhenova EN, Saris NE, Zvyagilskaya RA (2001) Ca(2+) efflux in mitochondria from the yeast *Endomyces magnusii*. J Biol Chem 276(51):47801–47806

Deryabina YI, Isakova EP, Shurubor EI, Zvyagilskaya RA (2004) Calcium-dependent non-specific permeability of the inner mitochondrial membrane is not induced in mitochondria of the yeast *Endomyces magnusii*. Biochem Mosc 69(9):1025–1033

Flohé L, Otting F (1984) Superoxide dismutase assays. Methods Enzymol 105:93–104

Guidot DM, McCord JM, Wright RM, Repine JE (1993) Absence of electron transport (Rho 0 state) restores growth of a manganese-superoxide dismutase-deficient *Saccharomyces cerevisiae* in hyperoxia. Evidence for electron transport as a major source of superoxide generation in vivo. J Biol Chem 268:26699–266703

Gulbins E, Dreschers S, Bock J (2003) Role of mitochondria in apoptosis. Exp Physiol 88:85–90

Gunter TE, Buntinas L, Sparagna G, Eliseev R, Gunter K (2000) Mitochondrial calcium transport: mechanisms and functions. Cell Calcium 28:285–296

Gunter TE, Yule DI, Gunter KK, Eliseev RA, Salter JD (2004) Calcium and mitochondria. FEBS Lett. 567:96-102

Hajnyczky G, Csordбs G, Das S, Garcia-Perez C, Saotome M, Sinha Roy S, Yi M (2006) Mitochondrial calcium signalling and cell death: approaches for assessing the role of mitochondrial Ca^{2+} uptake in apoptosis. Cell Calcium 40:553–560

Halliwell B, Aruoma OI (1991) Mitochondrial calcium signalling and cell death: approaches for assessing the role of mitochondrial Ca^{2+} uptake in apoptosis. FEBS Lett 281:9–19

Han D, Williams E, Cadenas E. (2001) Mitochondrial respiratory chain-dependent generation of superoxide anion and its release into the intermembrane space. Biochem. J 353:411–416

Hansford RG, Zorov D (1998) Role of mitochondrial calcium transport in the control of substrate oxidation. Mol Cell Biochem 184:359–369

Herrero E, Ros J, Bel G, Cabiscol E (2008) Redox control and oxidative stress in yeast cells. Biochim Biophys Acta 1780:1217–1235

Jung DW, Bradshaw PC, Pfeiffer DR (1997) Properties of a cyclosporin-insensitive permeability transition pore in yeast mitochondria. J Biol Chem 272:21104–21112

Kostyuk VA, Potapovich AI, Kovaleva JV (1990) A simple and sensitive method of determination of superoxide dismutase activity based on the reaction of quercetin oxidation. Vopr Med Chim 2:88–91

Kovaleva MV, Sukhanova EI, Trendeleva TA, Zyl'kova MV, Ural'skaya LA, Popova KM, Saris NE, Zvyagilskaya RA (2009) Induction of a non-specific permeability transition in mitochondria from *Yarrowia lipolytica* and *Dipodascus (Endomyces) magnusii* yeasts. J Bioenerg Biomembr 41(3):239–249

Kowaltowski AJ, Vercesi AE (1999) Mitochondrial damage induced by conditions of oxidative stress. Free Radic Biol Med 26:463–471

Kowaltowski AJ, Vercesi AE, Rhee SG, Netto LE (2000) Catalases and thioredoxin peroxidase protect *Saccharomyces cerevisiae* against Ca(2+)-induced mitochondrial membrane permeabilization and cell death. FEBS Lett 473:177–182

Kowaltowski AJ, de Souza-Pinto NC, Castilho RF, Vercesi AE (2009) Mitochondria and reactive oxygen species. Free Radic Biol Med 47:333–43

Kroemer G, Galluzzi L, Brenner C (2007) Mitochondrial membrane permeabilization in cell death. Physiol Rev 87:99–163

Lemasters JJ, Theruvath TP, Zhong Z, Nieminen AL (2009) Mitochondrial calcium and the permeability transition in cell death. Biochim Biophys Acta 1787:1395–1401

Leung AWC, Halestrap AP (2008) Recent progress in elucidating the molecular mechanism of the mitochondrial permeability transition pore. Biochim Biophys Acta 1777:946–952

Lledias F, Rangel P, Hansberg W (1998) Oxidation of catalase by singlet oxygen. J Biol Chem 273:10630–10637

Lopez-Mirabal HR, Winther JR (2008) Redox characteristics of the eukaryotic cytosol. Biochim Biophys Acta 1783:629–640

Lushchak VI (2011) Adaptive response to oxidative stress: bacteria, fungi, plants and animals. Comp Biochem Physiol C Toxicol Pharmacol 153:175–190

Matrosova EV, Masheyka IS, Kudryavtseva OA, Kamzolkina OV (2009) Morphogenesis and ultrastructure of basidiomycetes *Agaricus* and *Pleurotus* mitochondria. Cell and Tissue Biology 3(4):369–380

McCormack JG, Denton RM (1994) Signal transduction by intramitochondrial Ca^{2+} in mammalian energy metabolism. News Physiol Sci 9:71–76

Nicholls DG, Ferguson SJ (1992) Bioenergetics 2. Academic, San Diego

Ojovan SM, Knorre DA, Severin FF, Bakeeva LE (2009) Yeast cell ultrastructure after amiodarone treatment. Tsitologiya 51(11):911–916

Peng TI, Jou MJ (2010) Oxidative stress caused by mitochondrial calcium overload. Ann NY Acad Sci 1201:183–188

Perrone GG, Tan SX, Dawes IW (2008) Reactive oxygen species and yeast apoptosis. Biochim. Biophys Acta 1783:1354–1368

Rasola A, Bernardi P (2007) The mitochondrial permeability transition pore and its involvement in cell death and in disease pathogenesis. Apoptosis 12:815–833

Reynolds ES (1963) The use of lead citrate at high pH as an electron opaque strain in electron microscopy. J Biophys Biochem Cytol 17:208

Scherz-Shouval R, Elazar Z (2011) Regulation of autophagy by ROS: physiology and pathology. Trends Biochem Sci 36:30–38

Streiblova E (1988) Cytological methods. In: Campbell J, Buffers JM (eds) Yeast – A Practical Approach, IRL Press, Oxford, pp 9–49

Trendeleva T, Sukhanova E, Ural'skaya L, Saris NE, Zvyagilskaya R (2011a) Mitochondria from *Dipodascus (Endomyces) magnusii* and *Yarrowia lipolytica* yeasts did not undergo a Ca(2+)-dependent permeability transition even under anaerobic conditions. J Bioenerg Biomembr 43(6):623–631

Trendeleva T, Sukhanova E, Ural'skaya L, Saris NE, Zvyagilskaya R (2011b) Effect of pro-oxidants on yeast mitochondria. J Bioenerg Biomembr 43(6):633–644

Tsujimoto Y, Shimizu S (2007) Role of the mitochondrial membrane permeability transition in cell death. Apoptosis 12:835–840

van Loon AP, Pesold-Hurt B, Schatz G (1986) A yeast mutant lacking mitochondrial manganese-superoxide dismutase is hypersensitive to oxygen. Proc Natl Acad Sci USA 83:3820–3824

Yamada A, Yamamoto T, Yoshimura Y, Gouda S, Kawashima S, Yamazaki N, Yamashita K, Kataoka M, Nagata T, Terada H, Pfeiffer DR, Shinohara Y (2009) Ca^{2+}-induced permeability transition can be observed even in yeast mitochondria under optimized experimental conditions. Biochim Biophys Acta 1787:1486–1491